ATP-Dependent Substrate Occlusion by the Human Erythrocyte Sugar Transporter†

Karen S. Heard, Nancy Fidyk, and Anthony Carruthers*

Department of Biochemistry and Molecular Biology, University of Massachusetts Medical School, 55 Lake Avenue North, Worcester, Massachusetts 01655

Received August 18, 1999; Revised Manuscript Received December 8, 1999

ABSTRACT: Human erythrocyte sugar transport presents a functional complexity that is not explained by existing models for carrier-mediated transport. It has been suggested that net sugar uptake is the sum of three serial processes: sugar translocation, sugar interaction with an intracellular binding complex, and the release from this complex into bulk cytosol. The present study was carried out to identify the erythrocyte sugar binding complex, to determine whether sugar binding occurs inside or outside the cell, and to determine whether this binding complex is affected by cytosolic ATP or transporter quaternary structure. Sugar binding assays using cells and membrane protein fractions indicate that sugar binding to erythrocytes is quantitatively accounted for by sugar binding to the hexose transport protein, GluT1. Kinetic analysis of net sugar fluxes indicates that GluT1 sugar binding sites are cytoplasmic. Intracellular ATP increases GluT1 sugar binding capacity from 1 to 2 mol of 3-*O*-methylglucose/mol GluT1 and inhibits the release of bound sugar into cytosol. Reductant-mediated, tetrameric GluT1 dissociation into dimeric GluT1 is associated with the loss of ATP and 3-*O*-methylglucose binding. We propose that sugar uptake involves GluT1-mediated, extracellular sugar translocation into an ATP-dependent cage formed by GluT1 cytoplasmic domains. Caged or occluded sugar has three possible fates: (1) transport out of the cell (substrate cycling); (2) interaction with sugar binding sites within the cage, or (3) release into bulk cytosol. We show how this hypothesis can account for the complexity of erythrocyte sugar transport and its regulation by cytoplasmic ATP.

The facilitated diffusion of sugars across cell membranes is mediated by a family of integral membrane proteins called glucose transporters. Five mammalian glucose transporters have been identified (*1*). Of these transporters, the erythroid transporter GluT1[1] (*2*) has been studied most extensively with respect to structure (*3, 4*) and function (*5*).

The mechanism of GluT1-mediated glucose translocation is unknown. In the absence of stable GluT1−substrate intermediates for analysis, investigators have turned to the analysis of transport data in order to characterize intermediates in GluT1-mediated sugar transport. The earliest and most influential quantitative proposal resulting from this approach was the simple carrier hypothesis (*6*). According to this model, the transporter sequentially presents a sugar influx site (e_2) and then a sugar efflux site (e_1). Extracellular sugar binding to the influx site promotes a conformational change, resulting in the translocation of bound sugar to the cytosol and the creation of the sugar efflux site. Sugar binding to the efflux site promotes the reverse conformational change, causing translocation of sugar to the extracellular water and the regeneration of the sugar influx site. Conversion between e_1 and e_2 states in the absence of sugar occurs by a process called relaxation, but this is much slower than conversion in the presence of sugar (*7, 8*).

The simple carrier hypothesis was later modified to account for unequal affinities for glucose at the influx and efflux sites (*9*). Several groups have demonstrated that $K_{m(app)}$ and V_{max} for sugar efflux into sugar-free medium (zero-trans efflux) are 5−10-fold greater than $K_{m(app)}$ and V_{max} for sugar uptake into sugar-depleted cells (zero-trans uptake) (*7, 10−14*). An asymmetric simple carrier model can, in principle, account for this behavior (*9, 15*).

Baker and Widdas (*11*) proposed a fundamentally different model for erythrocyte glucose transport that was later termed the fixed-site carrier (*16*). According to this model, the transporter *simultaneously* presents a sugar efflux site *and* a sugar influx site. The fixed-site carrier is thus capable of forming an "extracellular sugar−carrier−intracellular sugar" ternary complex. Several studies from this laboratory demonstrate that the human erythrocyte sugar transporter presents e_1 and e_2 sites simultaneously (*14, 17−20*).

Analyses of the quaternary structure of GluT1 (*4, 19, 21*) demonstrate that the transporter is a complex of 4 GluT1 proteins. GluT1 reduction causes the transporter to dissociate into GluT1 dimers in which each GluT1 protein functions independently of its neighbor as a simple carrier and with lower catalytic turnover (*4, 19, 21*). GluT1 reduction may result in the loss of a single intramolecular disulfide bridge between GluT1 cysteine residues 347 and 421, which stabilizes GluT1 oligomeric structure (*4*). These observations

† This work was supported by NIH Grants DK 44888 and 36081.

* To whom correspondence should be addressed: e-mail anthony.carruthers@umassmed.edu; telephone 508 856 5570; FAX 508 856 6231.

[1] Abbreviations: GluT1, human erythrocyte glucose transport protein; 3OMG, 3-*O*-methylglucose; AMP−PCP, adenosine 5′-(β,γ-methylene)-triphosphate; AMP−PNP, 5′-adenylyl imidodiphosphate; ATP-γ-S, adenosine 5′-*O*-(3-thiotriphosphate); CCB, cytochalasin B; CCD, cytochalasin D; EDTA, ethylenediaminetetraacetic acid; HEPES, *N*-(2-hydroxyethyl)piperazine-*N*′-2-ethanesulfonic acid; RBC, red blood cell; SDS−PAGE, sodium dodecyl sulfate−polyacrylamide gel electrophoresis;Tris-HCl, tris(hydroxymethyl)aminomethane.

10.1021/bi991931u CCC: $19.00
Published on Web 02/15/2000

are consistent with target size analyses suggesting that GluT1 forms a tetramer in red cell membranes (*22*) and with freeze-fracture electron microscopy suggesting that GluT1 forms a dimer upon purification under reducing conditions (*23*). At this time, monomeric GluT1 has not been demonstrated physically in reconstituted or biological membranes. Some studies have suggested that octyl glucoside-solubilized, reduced, purified human GluT1 is monomeric (*24*). The significance of this is unclear, however, since detergents with short ($\leq$C8) alkyl chains are known to denature the native structure of the erythrocyte anion transporter while detergents with longer (C12) alkyl chains preserve transporter native structure (*25*).

Studies of GluT1 expressed in *Xenopus* oocytes indicate that Cys-less GluT1 is functional (*26*) and that wild-type GluT1 forms a reductant-insensitive, nontetrameric (possibly dimeric) state (*4*). It is not possible to state definitively that the catalytic turnover of wild-type and Cys-less GluT1 expressed in *Xenopus* oocytes approaches that observed for GluT1 in human red cells. Neither are data available to assess whether GluT1 expressed in *Xenopus* oocytes presents e1 and e2 sites simultaneously as in the red cell or, like reduced GluT1, functions as a simple carrier. However, these observations do establish that fundamental GluT1 function (sugar translocation) does not require GluT1 assembly into homotetramer.

These studies have lead to the suggestion that each GluT1 protein functions in isolation as a simple carrier but that cooperative interactions between GluT1 proteins within the GluT1 tetramer cause the transport complex to present two e_1 sites and two e_2 sites at any instant (*18, 19*).

It is certain, however, that neither the asymmetric simple carrier nor the fixed-site carrier can account for the steady-state sugar transport properties of human erythrocytes (*5, 14*). Unidirectional sugar efflux from red cells into medium containing saturating sugar levels is characterized by a $K_{m(app)}$ that is almost 1 order of magnitude lower than that predicted by either carrier mechanism (*10, 12, 14*). $K_{m(app)}$ for unidirectional 3-*O*-methylglucose (3OMG) uptake by red cells containing saturating 3OMG levels is significantly greater than $K_{i(app)}$ for extracellular 3OMG inhibition of net 3OMG exit (*27*). These and related observations have prompted Naftalin and co-workers (*12, 16, 28, 29*) to suggest that human erythrocyte sugar transport may be intrinsically symmetric but that intracellular sugar complexation or the presence of a cytosolic unstirred sugar layer just below the plasma membrane could give rise to inaccuracies in initial transport rate determinations, thereby leading to apparent transport asymmetry and complexity.

This hypothesis is supported by several observations. (1) Human erythrocyte sugar transport asymmetry can be reduced or even lost in red blood cell ghosts (*13, 30*−*36*). (2) GluT1-mediated sugar transport in rabbit erythrocytes, in metabolically poisoned pigeon erythrocytes, and in rat adipocytes is symmetric (*37*−*39*). Rat erythrocyte sugar transport has been reported to be either symmetric (*40*) or asymmetric (*41*). (3) Transport measurements in human erythrocytes indicate that the transporter is asymmetric while CCB binding measurements indicate transporter symmetry (*14*). (4) Not all intracellular D-glucose is freely diffusible in erythrocytes (*28, 29, 40, 42*). (5) Reconstituted, purified glucose transporter displays 1.4-fold catalytic asymmetry versus 5−10-fold asymmetry in situ (*8, 43*). (6) If transport were rate-limited by a cytosolic diffusion barrier, net sugar uptake or exit at low sugar concentrations ($\ll K_m$) should be a biexponential process reflecting the movement of sugar through two compartments in series. Our studies confirm this prediction and that red cells contain a high-affinity sugar binding complex (*42*). This lead to the proposal (*42*) that newly imported sugar interacts rapidly with an intracellular sugar binding complex from which it dissociates slowly into bulk cytosol. Subsequent studies from this laboratory (*44*) indicate that the binding complex is not the GluT1 binding protein glyceraldehyde phosphate dehydrogenase (*45*), nor is it a membrane constituent that interacts with GluT1 with high affinity.

In the present study, we set out to identify the component-(s) of the proposed erythrocyte sugar binding complex, to determine whether cytosolic ATP levels and transporter quaternary structure affect sugar binding to the sugar binding complex, and to determine whether the sugar binding sites are located within or outside the cell. Our findings suggest that the glucose transporter is the proposed sugar binding complex, that GluT1 oligomeric structure and intracellular ATP modulate the sugar binding properties of GluT1, and that the high-affinity sugar binding sites are located within an intracellular domain of GluT1.

MATERIALS AND METHODS

Materials. [^{3}H]-3-*O*-methylglucose, [^{14}C]-D-glucose, [^{14}C]-2-deoxy-D-glucose, [^{3}H]cytochalasin B, [^{14}C]sucrose, and [^{3}H]H_2O were purchased from New England Nuclear. Rabbit antisera raised against a synthetic carboxyl-terminal peptide of GluT1 (C-term Ab) were obtained from East Acres Biologicals. Recently expired human blood was obtained from the University of Massachusetts Medical Center Blood Bank, and recently drawn human blood was obtained from the Massachusetts Chapter of the Red Cross. Reagents were purchased from Sigma Chemical Co., Calbiochem, or Bio-Rad.

Solutions. Saline consisted of 150 mM NaCl, 5 mM HEPES, and 0.5 mM EDTA, pH 7.4. KCl medium consisted of 150 mM KCl, 5 mM HEPES, and 0.5 mM EDTA, pH 7.4. Lysis medium contained 10 mM Tris-HCl and 2 mM EDTA, pH 7.4. Tris medium consisted of 50 mM Tris-HCl and 2 mM EDTA, pH 7.4. Stripping solution consisted of 2 mM EDTA and 15.4 mM NaOH, pH 12.0. Stopper consisted of ice-cold saline or KCl medium plus 10 μM cytochalasin B and 100 μM phloretin. All cytochalasin B binding solutions contained 10 μM cytochalasin D in order to competitively inhibit cytochalasin B binding to actin and other non-GluT1 sites (*14*).

Red Cells. Red cells were isolated from whole human blood by repeated wash/centrifugation cycles in ice-cold saline. One volume of whole blood was mixed with 3 or more volumes of saline and centrifuged at 10000*g* for 5 min at room temperature. Serum and the buffy coat were aspirated and the wash/centrifugation cycle was repeated until the supernatant was clear and the buffy coat was no longer visible. Cells were resuspended in 20 volumes of saline and were incubated for 30 min at 37 °C in order to deplete intracellular sugar levels.

Red Cell Ghosts. Red cell ghosts were prepared by lysis of washed red cells in 50 volumes of ice-cold hypotonic lysis

medium for 10 min. Membranes were harvested by centrifugation at 27000*g* for 10 min and washed again in 50 volumes of lysis medium and centrifuged. Membranes were resealed in 20 volumes of KCl medium by incubation for 45 min at 37 °C. Resealed erythrocyte ghosts were pelleted by centrifugation at 27000*g* for 15 min and placed on ice. Ghosts containing ATP were prepared by resealing in KCl medium + 4 mM Mg·ATP.

Purified Glucose Transporter. GluT1 containing endogenous lipid was purified from human erythrocytes as described previously (*19*). Protein purity was verified by SDS−PAGE (*56*) and protein function by analysis of CCB binding capacity relative to protein content. Routinely, 20 mg of 95% purified glucose transporter was obtained from 1 unit of blood.

Zero-Trans 3-O-Methylglucose Uptake. 3OMG uptake was measured as described previously (*14*). Sugar-free cells or erythrocyte ghosts (at ice temperature) were exposed to 5 volumes of saline (ice temperature) containing variable concentrations of unlabeled sugar plus labeled sugar. Uptake was permitted to proceed over intervals as short as 5 s to intervals as long as 3 h, and then 50 volumes (relative to cell volume) of stopper solution was added to the cell suspension. Cells were sedimented by centrifugation (14000*g* for 30 s), washed once in stopper solution, collected by centrifugation and extracted in 500 μL of 3% perchloric acid. The acid extract was centrifuged and duplicate samples of the clear supernatant fluid were counted. Zero-time uptake points were prepared by addition of stopper solution to cells prior to addition of medium containing sugar and radiolabel. Cells were immediately processed. Radioactivity associated with cells at zero time was subtracted from the activity associated with cells following the uptake period. All uptakes were normalized to equilibrium uptake where cells were exposed to sugar medium at 37 °C for 60 min prior to addition of stopper solution. Uptake assays were performed with solutions and tubes preequilibrated to 4 °C. Triplicate or quadruplicate samples were processed at each time point.

Transport Determinations with Nonhydrolyzable ATP Analogues. Erythrocyte membranes were resealed with KCl medium lacking or containing 4 mM ATP, AMP−PCP, AMP−PNP, or ATPγS. Transport was allowed to proceed for 0, 0.5, or 60 min. Ghosts were then processed as described above.

Zero-Trans 3-O-Methylglucose Efflux. Cells were loaded with variable concentrations of 3OMG (0.01−40 mM) plus [^{3}H]-3OMG by incubation at 37 °C for 1 h. The cells were centrifuged, samples of the supernatant were counted, the residual supernatant was aspirated, and the cells were incubated on ice. Cells (20 μL, 80−90% hematocrit) were aliquoted into tubes (ice temperature) and dispersed in 20 mL of ice-cold saline. Under these conditions, the extracellular sugar transport sites ($K_{m(app)} = 0.3$ mM) are never more than 1% saturated with sugar at time zero. Samples were taken for cell counts by hemocytometer. Following incubation for an appropriate time interval, 1 mL of cell suspension was added to stopper solution, and the cells were pelleted by centrifugation and processed as described for uptake experiments. This allows for determination of exit rates by monitoring the loss of intracellular sugar. Cell samples were taken at 0, 30, 60, 180, and 300 s. At each time point, quadruplicate samples were processed.

Cytochalasin B Binding. Cytochalasin B binding to red cells or to purified glucose transporter was measured as described previously (*14*). Briefly, cells (30 μL of a 60−80% cell suspension) or GluT1 (50 μg of protein) were sedimented by centrifugation (1−10 min at 14000*g*) and the supernatant was aspirated. The pellet was resuspended by addition of 100 μL of medium containing [^{3}H]cytochalasin B. Aliquots (20 μL) of the suspension were mixed with 2 drops of H_2O_2 and were counted by liquid scintillation spectroscopy. This is a measure of "total" suspension [cytochalasin B]. Cells or GluT1 were incubated for 0.5−5 min on ice, by which time equilibrium cytochalasin B binding is achieved (*17*). The suspension was centrifuged at 14000*g* for 20−600 s and aliquots (20 μL) of the clear supernatant were counted by liquid scintillation spectroscopy. This is a measure of "free" [cytochalasin B]. Bound [cytochalasin B] is computed as total − free [cytochalasin B]. When binding was measured in cells containing D-glucose, cytochalasin B binding medium also contained an equimolar concentration of mannitol (to prevent cell lysis) or D-glucose. Cytochalasin B binding was also measured in sugar-free cells in the presence of mannitol or D-glucose or in the absence of extracellular sugar. Cytochalasin D (10 μM) was included in all solutions to inhibit CCB binding to non-GluT1 sites (*17*).

Equilibrium 3OMG Binding. Washed red blood cells, resealed red blood cell ghosts, alkali-stripped red blood cell membranes, or purified GluT1 was incubated with increasing amounts of unlabeled 3OMG (0−10 mM) and unlabeled sucrose (1 mM) for 45 min at 37 °C. [^{3}H]-3OMG and [^{14}C]sucrose were added to the reaction mixture, which was incubated for an additional 45 min at 37 °C. Membranes were sedimented at 122000*g* in a Beckman Airfuge, the supernatant was removed, and duplicate samples of the supernatant were counted by liquid scintillation spectrometry. The pellet was solubilized and counted for radioactivity and assayed for hemoglobin (RBC) or protein (ghosts and GluT1) concentration. [Hemoglobin] was measured by absorption spectroscopy at 417 nm. [Protein] was measured by the Pierce BCA assay. The equilibrium 3OMG pellet volume was calculated by subtracting the water space of the pellet (^{14}C) from the total tritium space of the pellet. Sample ^{14}C and ^{3}H content were obtained by dual isotope separation on a Beckman LS-6500 scintillation spectrometer. With erythrocytes, the sucrose space represents extracellular water only. With unsealed erythrocyte membranes and with purified GluT1, the sucrose space represents extra- and intracellular or proteoliposomal water [unmodified, purified GluT1 proteoliposomes are unsealed (*18*)]. The 3OMG volume of the pellet was normalized relative to pellet hemoglobin or protein content. The number of red cells or red cell ghosts present in the pellet was calculated by using standard hemoglobin versus cell number or protein versus cell number calibration curves generated in parallel experiments. Cell counts were made with a hemocytometer. 3OMG space per cell or per microgram of membrane protein was also expressed relative to the concentration of CCB binding sites present in each sample.

In experiments where the effects of maltose or CCB on 3OMG binding were determined, cells were preequilibrated with 100 μM 3OMG, 1 mM sucrose and trace amounts of [^{3}H]-3OMG and [^{14}C]sucrose as described above. Maltose

(0−100 mM) or CCB (0−40 μM) was added to the reaction mixture, which was allowed to reequilibrate for an additional 30 min. The amount of 3OMG bound was measured as above. In experiments where red cells or red cell ghosts were treated with DTT, washed cells or resealed ghosts were incubated with 20 mM DTT in 10 volumes of human saline or KCl medium for 30 min at 37 °C. Cells were centrifuged and subsequently assayed for 3OMG binding and 3OMG transport in the absence of DTT.

Calculation of Transport Constants. All constants were computed by direct curve-fitting procedures using nonlinear regression of untransformed (nonlinearized) data. The software package used was KaleidaGraph 3.08d (Synergy Software, Reading, PA). Radiolabeled sugar uptake (time course) data were fitted to a two-compartment equation:

$$\mathrm{cpm}_t = \mathrm{cpm}_0 + \mathrm{cpm}_1(1 - \mathrm{e}^{-k_1 t}) + \mathrm{cpm}_2(1 - \mathrm{e}^{-k_2 t})$$

where cpm_t and cpm_0 are the counts associated with the cells at time t and zero time, respectively, and cpm_1 and cpm_2 are equilibrium counts associated with cell compartments 1 and 2, respectively. k_1 and k_2 are first-order rate constants describing the rate of equilibration of compartments 1 and 2, respectively. Where only a single cellular compartment for sugar penetration was presented, this analysis provides unique solutions for cpm_1 and cpm_2 but produces statistically indistinguishable solutions for k_1 and k_2.

Simulations of time-course data were generated by fourth-order Runge−Kutta numerical integration using the software package STELLA Research 4.0.2 PPC (High Performance Systems, Inc., Hanover, NH).

Analytical Procedures. [Protein] was determined by the Pierce BCA procedure. SDS−slab (10%) PAGE of membrane proteins and GluT1 were performed as described previously (*36*). Western blot analysis of proteins using C-term antibody was as described in ref *36*.

RESULTS

Does ATP Affect Multiphasic Transport? Sugar import into human erythrocytes is a multiphasic process consisting of a rapid filling of a small compartment followed by a slower filling of a large compartment (*42*). Multiphasic uptake is also present in hypotonically lysed, resealed erythrocytes that contain only residual cytosol and buffered KCl medium (*42, 44*). Previous studies from this laboratory have shown that ATP binds to the glucose transporter and modulates its activity (*34, 36*). We were interested, therefore, to determine whether ATP also affects biphasic sugar uptake.

Figure 1A shows that intracellular ATP increases the size of the fast compartment in resealed human erythrocyte membranes by 2.0-fold. The size of the slow compartment is unaffected by ATP. ATP is without effect on the rate of filling of the fast compartment but inhibits the rate of filling of the slow compartment. ATP restores the size of the fast compartment to that of whole red blood cells (Figure 1B). Provided Mg·ATP is present during membrane resealing, the effect of ATP is observed whether or not Mg·ATP (4 mM) is present during the initial hypotonic lysis of red blood cells. This indicates that the absence or presence of ATP during lysis does not cause the quantitative elution of transport-modulating factors from the erythrocyte. The equilibrium 3OMG (10 mM) space of erythrocyte ghosts (65 ± 3 fL/erythrocyte ghost) is unaffected by inclusion of 4 mM Mg·ATP during resealing (volume = 66 ± 9 fL/erythrocyte ghost; $n = 6$).

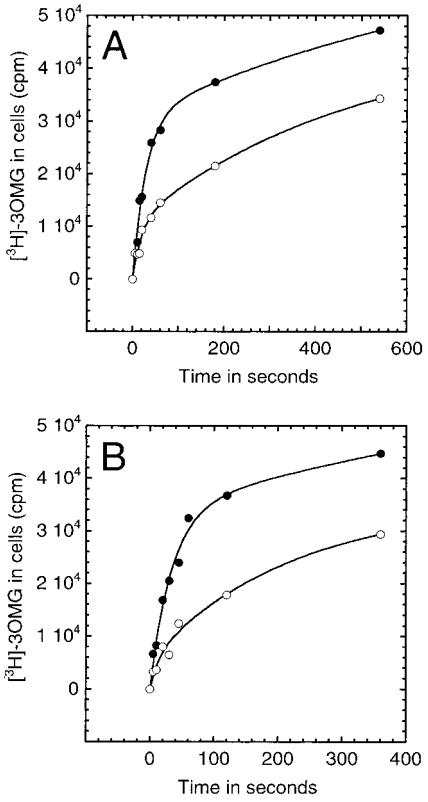

FIGURE 1: Time course of 3OMG uptake by erythrocyte ghosts (A) or by red blood cells (B). (A) Erythrocyte ghosts were resealed in the absence (○) or presence (●) of 4 mM ATP. 3OMG uptake at 50 μM 3OMG was assayed at ice temperature. Ordinate: [^{3}H]-3OMG associated with RBCs in counts per minute. Abscissa: time in seconds. Measurements were made in triplicate for each time point. Curves drawn through the points were computed by nonlinear regression assuming two exponents (see Materials and Methods). The constants obtained are as follows: +ATP, $\mathrm{cpm}_1 = 30\,712 \pm 4936$ cpm, $k_1 = 0.035 \pm 0.012$ s^{-1}; $\mathrm{cpm}_2 = 35\,433 \pm 5128$ cpm, and $k_2 = 0.0012 \pm 0.0006$ s^{-1}; −ATP, $\mathrm{cpm}_1 = 10\,501 \pm 3918$ cpm, $k_1 = 0.052 \pm 0.027$ s^{-1}, $\mathrm{cpm}_2 = 35\,149 \pm 1444$ cpm, and $k_2 = 0.0021 \pm 0.0002$ s^{-1}. (B) Red blood cells were incubated without (●) or with 20 mM DTT (○) for 30 min at 37 °C. Cells were then assayed for uptake of 50 μM 3OMG at ice temperature. Ordinate: [^{3}H]-3OMG associated with RBCs in counts per minute. Abscissa: time in seconds. Measurements were made in triplicate for each time point and are shown as the mean of five separate experiments. Curves drawn through the points were computed by nonlinear regression assuming two exponents. The constants obtained are as follows: control RBC, $\mathrm{cpm}_1 = 33\,930 \pm 2185$ cpm, $k_1 = 0.029 \pm 0.018$ s^{-1}, $\mathrm{cpm}_2 = 35\,361 \pm 5128$ cpm, and $k_2 = 0.0010 \pm 0.0006$ s^{-1}; RBC + DTT, $\mathrm{cpm}_1 = 5721 \pm 5106$ cpm; $k_1 = 0.073 \pm 0.047$ s^{-1}, $\mathrm{cpm}_2 = 29\,564 \pm 6129$ cpm, and $k_2 = 0.0045 \pm 0.0004$ s^{-1}. Number of cells per assay = 8.9×10^8. One microliter of [^{3}H]-3OMG (50 μM) = 603 cpm.

ATP modulation of the erythrocyte glucose transporter has been shown to be an allosteric effect that is independent of nucleotide hydrolysis (*34*). We therefore examined whether the action of ATP on the size of the fast compartment is dependent on nucleotide hydrolysis by comparing transport of 3OMG in ghosts lacking or containing ATP or several nonhydrolyzable ATP analogues. Uptake measurements made at 30 s (where ATP modulation of the fast compartment is greatest) show that nonhydrolyzable ATP analogues are as effective as ATP in increasing the size of the fast uptake

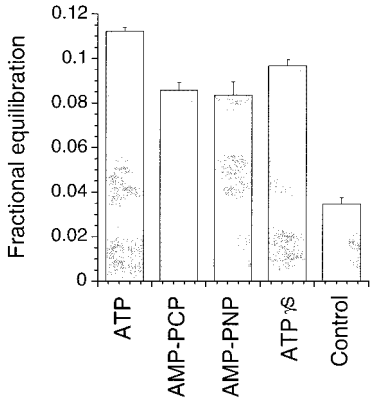

FIGURE 2: Effects of nonhydrolyzable ATP analogues on 3OMG uptake in erythrocyte ghosts. Ordinate: Fractional equilibration of red blood cell ghosts with 50 μM extracellular 3OMG measured at 30 s. Abscissa: resealing conditions, i.e., absence (control) or presence of 4 mM ATP, AMP−PCP, AMP−PNP, or ATPγS. Results represent the mean ± SEM of measurements made in triplicate or quadruplicate for each time point. Statistical analysis (two-tailed *t*-test) indicates that sugar uptake is significantly increased ($p < 0.05\%$) by ATP and its analogues. There is no significant difference between transport rates in ghosts containing AMP−PCP, AMP−PNP, and ATPγS ($p > 9.4\%$). Transport in ATP-containing ghosts is not significantly different from that in AMP−PCP-containing ghosts ($p > 50\%$) but is significantly greater than that observed in ghosts containing AMP−PNP and ATPγS ($p < 0.1\%$).

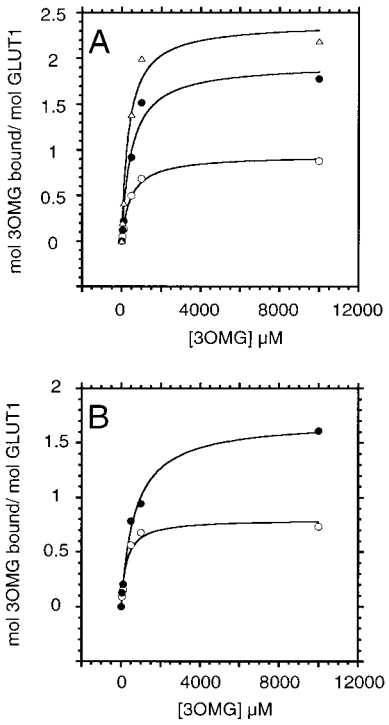

FIGURE 3: 3OMG binding activity of erythrocytes, erythrocyte ghosts, and purified GluT1. (A) Red blood cells (●) and red blood cell ghosts resealed in the presence (△) and absence (○) of 4 mM ATP were assayed for 3OMG binding by equilibrium 3OMG space analysis. Ordinate: moles of 3OMG bound per mole of GluT1. Abscissa: micromolar concentration of 3OMG. This plot summarizes at least four separate experiments made in triplicate. The curves drawn through the points were computed by nonlinear regression assuming that equilibrium 3OMG binding is described by the expression [3OMG bound] = B_{max}[3OMG]/{$K_{d(app)}$ + [3OMG]}, where B_{max} is 3OMG binding capacity and $K_{d(app)}$ is that [3OMG] where [3OMG bound] = 0.5B_{max}. The curves have the following constants: RBC , $B_{max} = 1.93 \pm 0.15$ mol of 3OMG bound/mol of GluT1 and $K_{d(app)} = 475 \pm 126$ μM 3OMG; ghosts + ATP, $B_{max} = 2.38 \pm 0.16$ mol of 3OMG bound/mol of GluT1 and $K_{d(app)} = 344 \pm 83$ μM 3OMG; ghosts − ATP, $B_{max} = 0.94 \pm 0.4$ mol of 3OMG bound/mol of GluT1 and $K_{d(app)} = 458 \pm 67$ μM 3OMG. (B) Purified GluT1 was assayed for 3OMG binding in the presence (●) and absence (○) of 4 mM ATP. Ordinate: moles of 3OMG bound per mole of GluT1. Abscissa: micromolar concentration of 3OMG. This plot summarizes at least four separate experiments made in triplicate. The curves drawn through the points were computed by nonlinear regression assuming that equilibrium binding is described by the expression [3OMG bound] = B_{max}[3OMG]/{$K_{d(app)}$ + [3OMG]} and have the following constants: GluT1 + ATP, $B_{max} = 1.71 \pm 0.06$ mol of 3OMG bound/mol of GluT1 and $K_{d(app)} = 689 \pm 76$ μM 3OMG; GluT1 − ATP, $B_{max} = 0.80 \pm 0.05$ mol of 3OMG bound/mol of GluT1 and $K_{d(app)} = 269 \pm 69$ μM 3OMG.

compartment (Figure 2). This indicates that ATP modulation of the fast uptake compartment is independent of ATP hydrolysis.

Is Multiphasic Transport Dependent on Transporter Oligomeric Structure? Hydrodynamic analyses indicate that GluT1 forms a homotetramer in the erythrocyte membrane that dissociates into dimers upon exposure to extracellular reductant (*4*, *19*). DTT also inhibits ATP modulation of 3OMG uptake in erythrocyte ghosts and inhibits azido-[γ-^{32}P]ATP incorporation into GluT1 (*36*). If GluT1 tetrameric structure is necessary for ATP modulation of GluT1, we would predict that treatment of red blood cells with extracellular reductant should reduce the size of the fast compartment through loss of ATP binding. Figure 1B shows that DTT treatment of erythrocytes reduces the size of the fast uptake compartment by 2.2-fold and produces a proportional increase in the size of the slow uptake compartment. This result is consistent with the previous findings indicating that tetrameric GluT1 but not dimeric GluT1 is modulated by ATP (*36*).

What Cellular Components Form the Sugar-Binding Complex? This laboratory has proposed that multiphasic sugar uptake results from saturable sugar binding within the cell (*42*). Equilibrium 3OMG uptake experiments demonstrate saturable 3OMG binding to human erythrocytes (Figure 3 and see ref *42*). We therefore set out to identify those red blood cell component(s) that comprise the 3OMG binding complex. The strategy we adopted was to assay for the loss of erythrocyte 3OMG binding activity as erythrocyte membranes progress through the GluT1 purification protocol. In this way we could identify which fraction of the erythrocyte contains the sugar binding activity—cytosol, peripheral membrane proteins, or integral membrane proteins.

To measure sugar binding during each step of GluT1 purification, it was necessary to develop a 3OMG binding assay that would provide sufficient sensitivity to measure sugar binding in lysed cells and in unsealed proteoliposomes. Erythrocyte shape and density facilitate red cell packing during centrifugation and allow formation of a cell pellet in which more than 90% of the extracellular water is excluded. Erythrocyte ghosts and proteoliposomes pack less efficiently during centrifugation and a substantial portion of extracellular or extravesicular water remains. We therefore sedimented cells and membranes at 122000*g* using a Beckman Airfuge. We also employed a dual isotope procedure allowing measurement of both the water ([^{14}C]sucrose) space and 3OMG ([^{3}H]-3OMG) space of the pellet. By subtracting the water space (^{14}C) from the 3OMG space (^{3}H), we calculate

Table 1: 3OMG Binding Properties of Erythrocytes

membrane fraction	mol of 3OMG bound/ mol of GluT1[a]	
	0 ATP	+ATP
intact erythrocytes		1.93 ± 0.15[b]
DTT-treated erythrocytes		0.55 ± 0.03[c]
resealed erythrocyte ghosts	0.94 ± 0.04	2.38 ± 0.16[d]
integral membrane proteins	1[e]	
purified GluT1	0.80 ± 0.05	1.71 ± 0.06

[a] 3OMG binding was expressed relative to the GluT1 content of human erythrocytes or erythrocyte membrane fractions as measured by CCB binding capacity (e.g., see Figure 3). We assumed that 1 mol of GluT1 binds 0.5 mol of CCB (see refs *18* and *19*). If 1 mol of GluT1 binds 1 mol of CCB, all numbers in this table must be factored by 2. [b] We assume red cells contain 2−4 mM ATP (*33*). [c] Red cells were treated with DTT but binding was expressed relative to the CCB binding capacity of control RBCs. $K_{d(app)}$ for 3OMG binding to DTT-treated cells = 426 ± 392 μM 3OMG. The binding capacity of control RBCs in these experiments is 1.48 ± 0.38 mol of 3OMG/mol of GluT1. [d] Red cell ghosts contained 4 mM Mg·ATP. [e] This experiment was performed once. All other measurements were made three time in triplicate. Results are shown as mean ± SEM.

specific 3OMG binding space and in this way increase the signal-to-noise ratio of each determination. Intracellular water in red cells and resealed ghosts is inaccessible to sucrose.

Resealed erythrocyte ghosts demonstrate saturable 3OMG binding (Figure 3A) and biphasic 3OMG uptake (Figure 1A). The 3OMG binding capacity of ghosts, however, is approximately half that of whole red cells (Figure 3A). If the size of the ATP-sensitive, fast uptake compartment is related to the 3OMG binding capacity of the cell, the 3OMG binding capacity of the cell may also be sensitive to cytosolic ATP. Figure 3A demonstrates that the 3OMG binding capacity of erythrocyte ghosts is restored to levels observed in red blood cells when erythrocyte ghosts are resealed in the presence of ATP. We propose, therefore, that ATP modulates 3OMG binding to the erythrocyte membrane.

We next depleted erythrocyte membranes of peripheral membrane proteins by washing erythrocyte ghosts in a high-pH solution (*46*). The remaining integral membrane proteins are capable of binding 3OMG to a level similar to that observed in erythrocyte ghosts lacking ATP (Table 1). Finally, we tested the ability of the purified erythrocyte glucose transport protein to bind 3OMG. Purified GluT1 is a 3OMG binding protein and addition of ATP restores GluT1−3OMG binding to a level observed in red blood cells (Figure 3B). The stoichiometry of GluT1 sugar binding is close to 2 mol of 3OMG/mol of GluT1.

Tetrameric GluT1 binds ATP with $K_{d(app)}$ of 300−500 μM (*36*). ATP increases GluT1 3OMG binding capacity in a saturable manner with half-maximal effects at 679 ± 364 μM (Figure 4).

If the rapid filling of the small uptake compartment seen in transport measurements represents transport-limited, rapid binding of 3OMG to the sugar binding sites of GluT1, then 3OMG binding to GluT1 should be inhibited by reductant just as the size of the fast compartment is reduced by DTT. 3OMG binding capacity of red cells is decreased by extracellular reductant (Table 1).

Are the 3OMG Binding Sites Intracellular or Extracellular? By making the simplifying assumption that 3OMG binding sites approximate an unstirred layer of sugar, it is possible to determine whether the unstirred layer is present inside or outside the cell (*9*). This method requires that the initial rate of transport (v) is determined over a wide range of sugar levels [S] and represented graphically as [S]/v versus [S]. At high [S], the data fall on a single straight line with a slope $1/V_{max}$. If a significant cis-unstirred layer exists (inside and outside the cell for exit and uptake experiments, respectively), the data points at low [S] deviate upward from the fit obtained from the data points at higher [S] because the concentration of sugar in the space between the transporter and the diffusion barrier, $[S]_{membrane}$, is significantly lower than that in the bulk solution beyond the diffusion barrier. Red cell 3OMG exit data are well approximated by a Michaelis−Menten curve (Figure 5A). However, when the exit data are expressed as [S]/v versus [S] (Figure 5B), they are linear over the [3OMG] range 2.5−14 mM but deviate from linearity over the [3OMG] range 0−2.5 mM. This deviation exceeds the computed 95% confidence interval for the least-squares extrapolation of data at higher [3OMG]. This suggests the presence of an unstirred layer inside the cell. The permeability coefficient for 3OMG flux across this cytosolic barrier is obtained as the reciprocal of the difference between the extrapolated least-squares *y*-intercept of Figure 5B and the observed *y*-intercept. In this experiment the rate constant for sugar diffusion of across this barrier is 0.3 min^{-1}, which is in close agreement with the rate of filling of the slow uptake compartment of red blood cells (0.26 ± 0.10 min^{-1}; Figure 1).

Zero-trans uptake experiments were also performed (Figure 5). When the uptake data are expressed as [S]/v versus [S], they show linearity over the entire [3OMG] range (0−10 mM). This suggests that there is no unstirred layer at the extracellular side of the cell.

To further test this hypothesis, we examined the effects of maltose and CCB for their ability to modulate 3OMG

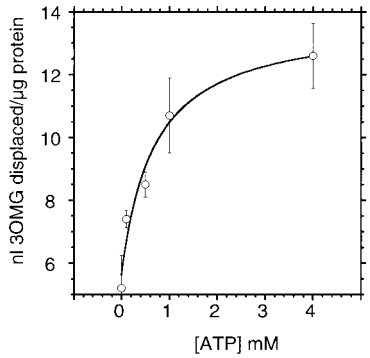

FIGURE 4: ATP concentration dependence of 3OMG binding in erythrocyte ghosts. Red blood cell ghosts were resealed in increasing amounts of ATP. 3OMG equilibrium space analysis was assayed at 0 and 10 mM 3OMG. Ordinate: nanoliters per microgram of protein 3OMG binding space displaced by 10 mM 3OMG. Abscissa: millimolar ATP concentration. Results represent the mean ± SEM of at least three separate experiments performed in triplicate. The curve drawn through the points was computed by nonlinear regression assuming that binding is described by the expression [3OMG bound] = $b_0 + \Delta_{ATP}[ATP]/\{K_{ATP} + [ATP]\}$. b_0 is 3OMG binding in the absence of ATP, Δ_{ATP} is the increase in 3OMG binding (over b_0) produced by saturating [ATP], and K_{ATP} is that concentration of ATP increasing 3OMG binding by $0.5\Delta_{ATP}$. The curve drawn though the points has the following constants: b_0 = 5.6 ± 0.6 nL/μg of protein 3OMG binding space; Δ_{ATP} = 8.2 ± 1.3 nL/μg of protein 3OMG binding space; $K_{0.5}$ = 679 ± 364 μM ATP.

binding to erythrocytes. Maltose is a nontransportable inhibitor of erythrocyte sugar transport that interacts with the GluT1 sugar uptake site, whereas CCB is a competitive inhibitor of erythrocyte sugar efflux and is presumed to interact with the GluT1 sugar exit site (*20*). Cells were first equilibrated with 100 μM 3OMG and then increasing concentrations of maltose and CCB were added to displace bound 3OMG. CCB inhibits 3OMG binding in erythrocytes (maximum inhibition $I_{max} = 15.80 \pm 1.63$ fL/erythrocyte; $K_{i(app)} = 1.65 \pm 0.65$ μM CCB; $n = 3$). Maltose also inhibits 3OMG binding to erythrocytes ($I_{max} = 10.63 \pm 1.54$ fL/erythrocyte; $K_{i(app)} = 1.16 \pm 0.57$ mM; $n = 3$).

DISCUSSION

The present study demonstrates that high-affinity sugar binding to human erythrocytes results from sugar binding to the hexose transport protein, GluT1. Kinetic analysis of net sugar fluxes indicates that GluT1 sugar binding sites are cytoplasmic. Intracellular ATP increases GluT1 sugar binding capacity from 1 to 2 mol of 3-*O*-methylglucose/mol of GluT1 and inhibits the release of bound sugar into cytosol. Reductant-mediated, tetrameric GluT1 dissociation into dimeric GluT1 is associated with the loss of ATP and 3-*O*-methylgucose binding. These results are consistent with the hypothesis that 3OMG uptake by human erythrocytes is a three-step process: (1) GluT1-mediated sugar translocation, (2) sugar release into an internal transporter space or cage containing high-affinity sugar binding sites, and (3) release from this space or cage into cytosol.

Sugar Binding and Biphasic Sugar Uptake Reflect a Single ATP-Dependent Process. Cloherty et al. (*42*) have proposed that high-affinity sugar binding to an erythrocyte sugar binding complex is responsible for biphasic sugar uptake by red cells at low sugar concentrations. The results of the present study provide additional support for this hypothesis. Earlier observations are repeated, demonstrating that extracellular sugar rapidly fills a small cellular compartment ($k = 0.02-0.05$ s^{-1}, fractional cell 3OMG space = 0.4) and then slowly fills the bulk cytosol ($k = 0.0015$ s^{-1}, fractional cell 3OMG space = 0.6). Removal of intracellular ATP reversibly reduces the size of the fast uptake compartment 2-fold and reversibly reduces the 3OMG binding capacity of erythrocytes. This effect of ATP on biphasic sugar uptake and cellular 3OMG binding does not require ATP hydrolysis and is half-maximal at 300−500 μM intracellular ATP. Finally we show that inhibition of ATP binding to the glucose transporter by GluT1 reduction using extracellular reductant (*36*) reduces by 2-fold both the size of the fast uptake compartment and the 3OMG binding capacity of erythrocytes. This suggests that the ATP-sensitive glucose transporter mediates both cellular sugar binding and biphasic sugar transport.

If erythrocyte ghosts resealed in the absence of ATP were larger than ATP-containing ghosts, this could result in an apparent increase in the size of the slow compartment (bulk cytosol) with a proportional decrease in the size of the fast compartment (sugar binding). This might occur, for example, if ATP were needed to maintain the cytoskeletal network and thus the shape and volume of the red cell (*47*). Sheetz and Singer (*48*) have shown that erythrocyte ghosts undergo a shape change upon resealing with Mg·ATP which is

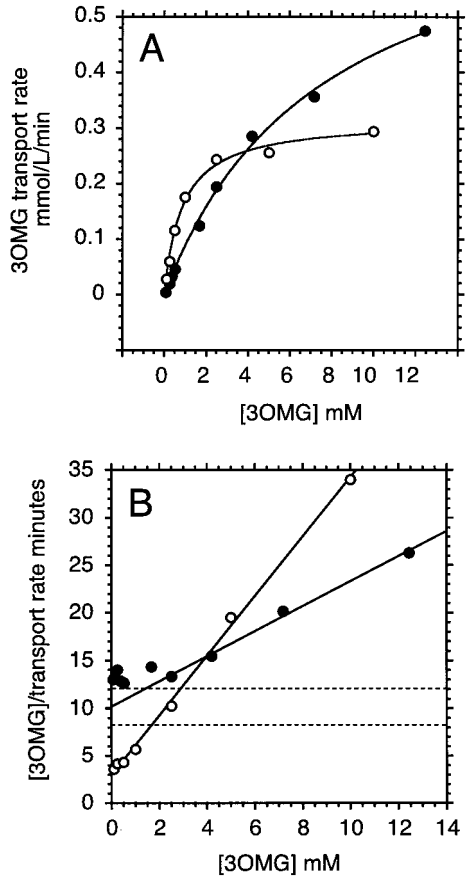

FIGURE 5: Is the barrier to sugar movements inside or outside the cell? (A) Concentration dependence of zero-trans 3OMG exit (●) or zero-trans entry (○) was measured in red blood cells loaded with or exposed to (respectively) varying concentrations of 3OMG. Ordinate: rate of 3OMG exit or entry in millimoles per liter of cell water per minute. Abscissa: millimolar concentration of 3OMG. These plots summarize five separate experiments performed in triplicate. The curves drawn through the data were computed by nonlinear regression analysis assuming that sugar transport, v, is described by $v = V_{max}[3OMG]/\{K_{m(app)} + [3OMG]\}$, where V_{max} is the maximum rate of sugar transport and $K_{m(app)}$ is that [3OMG] where $v = 0.5V_{max}$. The following parameters were obtained: exit (●), $K_{m(app)} = 8.20 \pm 0.97$ mM and $V_{max} = 0.79 \pm 0.05$ mmol (L of cell water)$^{-1}$ min^{-1}; entry (○), $K_{m(app)} = 0.87 \pm 0.09$ mM and $V_{max} = 0.32 \pm 0.01$ mmol (L of cell water)$^{-1}$ min^{-1}. (B) Hanes−Woolf transformation of exit and entry data. Ordinate: concentration of [3OMG] divided by rate of 3OMG efflux (●) or entry (○) in minutes. Abscissa: millimolar concentration of 3OMG. The lines drawn through the points represent least-squares analysis of the data points at the four highest concentrations of 3OMG. The two dashed lines represent the 95% confidence limits for the *y*-intercept of the exit data.

dependent on ATP hydrolysis (AMP−PNP does not mimic the effect of ATP) and which does not result in altered ghost volume. The present study measures no significant erythrocyte ghost volume change upon resealing with ATP and demonstrates that AMP−PNP is effective in modulating the size of the fast compartment. We conclude, therefore, that ATP-dependent changes in the fast and slow sugar uptake compartments of erythrocyte ghosts are unrelated to erythrocyte volume changes.

The Glucose Transporter Is the ATP-Dependent Sugar-Binding Complex. Several lines of evidence suggest that the glucose transporter is the sugar-binding complex of human erythrocytes. (1) ATP binding to GluT1 is inhibited by reductant (*36*). This is thought to reflect reductant-promoted

tetrameric GluT1 dissociation into dimeric GluT1 (*19*). Exposure to reductant also halves the 3OMG binding capacity of red cells and the size of the fast uptake compartment—two effects mimicked by ATP omission in erythrocyte ghosts. (2) ATP doubles the 3OMG binding capacity of purified GluT1 to that level observed in intact cells and in erythrocyte ghosts containing ATP. (3) ATP binding to GluT1 (*36*), ATP modulation of GluT1-mediated transport (*49*), and ATP modulation of the size of the fast uptake compartment are half-maximal at 300−500 μM ATP and do not require nucleotide hydrolysis. (4) 3OMG binding to isolated GluT1 quantitatively accounts for 3OMG binding to human erythrocytes.

GluT1 Sugar Binding Sites Are Cytosolic. Analysis of the concentration dependence of net 3OMG uptake and exit indicate an intracellular barrier to sugar movements between the bulk cytosol and the sugar efflux site. An equivalent extracellular barrier was not observed. A similar asymmetric barrier has been reported for sugar movements in rat erythrocytes (*29, 40*). This result is not surprising in view of the strong correlation between the size of the fast uptake compartment and the sugar-binding capacity of the cell. If the binding sites were located at the extracellular surface, it is extremely unlikely that their contribution to biphasic sugar uptake would be detectable since bound extracellular sugar would be lost during post uptake processing of cells.

Cytochalasin B (a ligand that binds at or close to the sugar efflux site) displaces 3OMG from erythrocyte sugar binding sites. Surprisingly, extracellular maltose (a ligand that binds to the sugar uptake site) has a similar effect. These results are not directly related to sugar transport inhibition because adequate incubation times were used to ensure equilibrium sugar (100 μM) distribution between cytosol and interstitium prior to and after addition of inhibitors (control conditions, $k_{(app)}$ for 3OMG equilibration $= V_{max}/K_m \approx 0.5$ s^{-1}; $t_{0.5} =$ 1.4 s at 24 °C; for a cell in which transport is 99% inhibited, $k_{(app)} \approx 0.005$ s^{-1}; $t_{0.5} = 140$ s at 24 °C).

It is unclear whether the sugar binding sites measured in this and previous (*42, 44*) studies represent catalytic (transport) or noncatalytic sites. It is possible that CCB and 3OMG compete for binding at the same intracellular (export) site. If this were the case, however, GluT1 CCB and 3OMG binding capacities would be identical. In fact nonreduced GluT1 CCB binding capacity [0.5 mol of CCB/mol of GluT1 (*18, 19*)] is half the CCB binding capacity of reduced GluT1 (*19, 50*−*52*) and is one-fourth the GluT1 3OMG binding capacity. GluT1 CCB binding capacity is less than unity because only two subunits of any GluT1 tetramer expose a CCB binding (export) site at any time (*18, 19*). The remaining two subunits of the GluT1 tetramer present sugar import sites (*18, 19*) which, owing to their location, cannot contribute to the 3OMG binding reported here. It is possible, therefore, that the larger cytochalasin B molecule when bound at the sugar export site sterically inhibits 3OMG binding at ATP-sensitive (noncatalytic) sugar binding sites. To account for the effect of extracellular maltose, this model requires that the transporter undergo a conformational change upon interaction with extracellular maltose that results in the allosteric inhibition of 3OMG binding at intracellular, noncatalytic sites. In the absence of direct evidence, this remains speculative. Differential labeling of GLUT1 using reactive sugars may help to determine whether new (non-

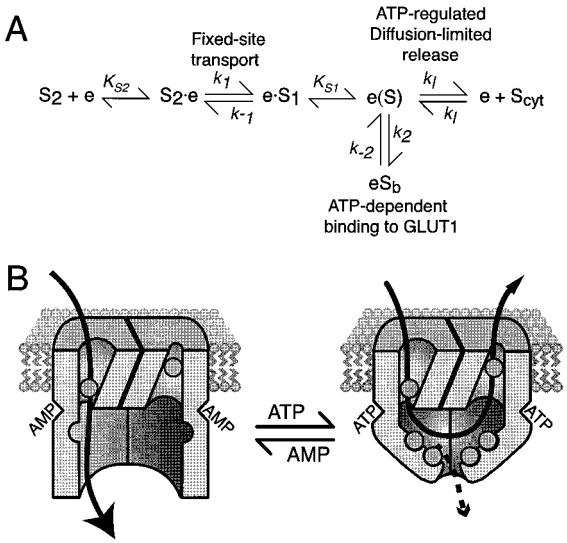

FIGURE 6: Model for GluT1 mediated sugar transport. (A) King−Altman schematic summarizing the steps involved in transport. Extracellular sugar (S2) interacts with the import site of a symmetric fixed-site carrier, is translocated and released into an occluded (intra-GluT1) water filled space. Occluded sugar e(S) can (1) recombine with the export site (to form eS1) and undergo export to the interstitium; (2) interact with either of two sugar binding sites presented by each GluT1 protein within the water filled space to form a noncatalytic e·Sb complex, or (3) be released into bulk cytosol (Scyt). The number of sugar binding sites and release into cytosol are affected by ATP. The data of Figure 1A can be mimicked by this scheme by assuming the following constants: +ATP, $K_{S2} = K_{S1} = 300$ μM, $V_{max} = [GluT1]k_1 = [GluT1]k_{-1} =$ 650 μmol (L of cell water)$^{-1}$ min^{-1}, $k_2 = 3$ μM^{-1} min^{-1}, $k_{-2} =$ 300 min^{-1}, $k_l = 0.08$ min^{-1}; n (number of binding sites) $= 3$, [GluT1] $= 20$ μM, and occluded volume $= 0.01$ cell volume. 0 ATP, as for +ATP with the following changes: $k_l = 0.04$ min^{-1} and n (number of binding sites) $= 0.6$. (B) Diagrammatic representation of this model. The figure to the left shows a section through the catalytic region of one dimer of tetrameric GluT1 embedded in a lipid bilayer and viewed from the plane of the bilayer. In the absence of ATP or when AMP is bound to GluT1, tetrameric GluT1 contains only one sugar binding site per monomer and newly imported sugar has facile access to bulk cytosolic water. Upon ATP binding (right), a conformational change occurs that restricts diffusion of sugar to and from the cytosol (a water-filled cage is formed) and exposes another sugar binding site per monomer. Under these conditions, a newly imported sugar has high probability of being exported back out of the cell or reacting with the sugar binding site. When tetrameric GluT1 is reduced to dimeric GluT1 by exposure to extracellular DTT, the ATP binding site is lost, the cage relaxes, and a sugar binding site is lost.

catalytic) sugar binding domains are generated upon GluT1 interaction with ATP.

A Model for GluT1-Mediated Transport. Figure 6 presents a model for sugar transport. The transporter (a kinetically symmetric GluT1 tetramer) undergoes a significant conformational change when ATP is bound. This conformation presents two, intracellular noncatalytic sugar binding sites per GluT1 subunit that are exposed at the interior of a "water-filled cage" formed by GluT1 cytoplasmic domains. Extracellular sugar reacts with either of two import subunits of the transporter and is translocated and released into this cage. The newly imported but "occluded" sugar then has three possible fates: (1) reassociation with export sites and translocation back into the interstitium (ATP-dependent substrate cycling), (2) slow release from the cage into bulk cytosol, or (3) interaction with and binding to noncatalytic sugar binding sites presented by the cage. ATP dissociation,

AMP competitive displacement of ATP, or loss of ATP binding sites by carrier dissociation into dimers results in the loss of noncatalytic sugar binding sites and the relaxation of the water-filled cage. A sugar newly imported by a relaxed carrier now has a high probability of entering bulk cytosol.

The present study demonstrates that GluT1 is an ATP-dependent sugar binding protein. The ATP-dependent conformational change/cage hypothesis is supported by three observations: (1) ATP binding to GluT1 inhibits anti-GluT1 C-terminal peptide antibody (C-Ab) binding to GluT1 (*34*). (2) AMP competitively displaces ATP from GluT1 and reverses the effect of ATP on C-Ab binding (*34*). (3) ATP protects intracellular GluT1 loops from proteolytic digestion.[2]

Predictions of Substrate-Cycling Model. This model makes several predictions that are consistent with available experimental findings. Sugar uptake at low [sugar] is biphasic and the size of the rapid phase of uptake (which represents sugar binding to noncatalytic GluT1 sites) is reduced in the absence of ATP (see Figure 1). When the carrier water filled cage is relaxed (ATP is depleted or the transporter is reduced to a dimer), transport should be kinetically symmetric. This is observed experimentally in human and avian erythrocytes (*8, 13, 30*−*36, 38, 43*). During sugar uptake measurements when the cage is closed, sugar levels within the cage will rise rapidly. This will cause significant sugar backflux (ATP-dependent substrate cycling) leading to underestimation of sugar uptake relative to exit ($V_{max}^{entry} < V_{max}^{exit}$). This is observed experimentally (*7, 10*−*14*). During net uptake, the increase in cage [sugar] will lead to significant underestimation of intracellular sugar levels required to inhibit saturated net sugar uptake by half ($K_{m(app)}$ infinite-cis uptake is anomalously low). This is observed experimentally (*10, 12, 14*). During net exit, slow equilibration between bulk cytosol and the interior of the cage will result in overestimation of cage [sugar] and, therefore, $K_{m(app)}$ for exit (exit is fast relative to sugar movement into the cage). Relaxation of the cage will thus result in decreased $K_{m(app)}$ for exit. This is observed experimentally (*13, 53*). ATP should be without effect on V_{max} for exchange transport (where intracellular [sugar] = extracellular [sugar]), because no transmembrane sugar gradient exists and the noncatalytic sugar binding sites are saturated with sugar. This prediction is also observed (*14, 34, 53*). Thus transport can be mediated by an intrinsically symmetric fixed-site carrier but substrate cycling, resulting from both sugar occlusion and sugar binding within the ATP-dependent cage, gives rise to anomalous transport behavior.

As we considered each of these issues, a concern remained that GluT1-mediated sugar transport in some tissues displays experimental, catalytic symmetry (see introduction). One fundamental difference between human erythrocytes and these other GluT1-expressing cells is the level of GluT1 expression. Human red cells are characterized by 100-1000-fold greater cell surface GluT1 density relative to avian, rabbit, or rat erythrocytes or rat adipocytes. Where it has been measured in these tissues, sugar uptake is monoexponential (*40, 54*). This reflects the obvious fact that sugar binding to GluT1 in these cells contributes less than 1% of the total equilibrated cellular 3OMG space if uptake is measured from media containing low sugar levels (e.g., 50 μM). We therefore simulated transport (according to the model of Figure 6) but in an ideal cell containing 500-fold fewer GluT1 proteins than human red cells. The result is that transport at low sugar concentrations is monoexponential but is operationally kinetically asymmetric. Thus symmetric, GluT1-mediated sugar transport cannot be explained simply by cellular GluT1 content. If the model of Figure 6 is correct, symmetric GluT1-mediated transport implies that the cage is opened either because cells are ATP-depleted [e.g., as in human and avian red cells (*13, 38, 53*)], because the transporter is a GluT1 dimer (and thus cannot bind ATP), or because other cellular factors or conditions prevent ATP-induced GluT1 conformational changes. Indirect evidence in support of the latter hypothesis is available from studies indicating that GluT1-mediated sugar transport in CHO cells [where GluT1 is tetrameric (*4*)], in K562 cells and in basal (non-insulin-treated) adipocytes is unaffected by ATP depletion (*4, 42, 55*).

The question arises as to whether ATP regulation of sugar occlusion is sufficient to account for ATP regulation of net sugar transport or whether ATP regulation of sugar translocation steps is also required. Our simulations of transport (see above) indicate that only V_{max} for net sugar uptake is reduced by substrate occlusion (V_{max} for exit and exchange transport is not significantly affected). However, one can envisage a situation where initial rates of transport are seriously underestimated through the use of extended incubation intervals of 30 s or greater. Here, the release of occluded substrate into cytosol (rather than initial binding of sugar to occlusion sites) becomes rate-limiting for net accumulation of sugar. The consequence of this will be to seriously underestimate the time course of sugar uptake or exit, resulting in a rate constant for transport approaching that for the release of occluded sugar. This will suggest strong transport inhibition under conditions where sugar translocation is unimpaired.

CONCLUSION

The human erythrocyte sugar transporter undergoes a conformational change upon binding ATP that reveals two noncatalytic sugar binding sites on each GluT1 protein and reduces the rate of release of bound sugar into cytosol. This behavior explains why previous carrier models have been unable to account for erythrocyte sugar transport kinetics and provides a basis for ATP regulation of transport.

REFERENCES

1. Mueckler, M. (1994) *Eur. J. Biochem. 219*, 713−25.
2. Mueckler, M., Caruso, C., Baldwin, S. A., Panico, M., Blench, I., Morris, H. R., Allard, W. J., Lienhard, G. E., and Lodish, H. F. (1985) *Science 229*, 941−945.
3. Hresko, R. C., Kruse, M., Strube, M., and Mueckler, M. (1994) *J. Biol. Chem. 269*, 20482−8.
4. Zottola, R. J., Cloherty, E. K., Coderre, P. E., Hansen, A., Hebert, D. N., and Carruthers, A. (1995) *Biochemistry 34*, 9734−47.
5. Carruthers, A., and Zottola, R. J. (1996) Transport Processes in Eukaryotic and Prokaryotic Organisms, in *Handbook of Biological Physics.* (Konings, W. N., Kaback, H. R., and Lolkema, J. S., Eds.) pp 311−342, Elsevier, Amsterdam.
6. Widdas, W. F. (1952) *J. Physiol. (London) 118*, 23−39.
7. Lowe, A. G., and Walmsley, A. R. (1986) *Biochim. Biophys. Acta 857*, 146−154.

[2] K. B. Levine, E. K. Cloherty, S. Hamill, and A. Carruthers, 1999, unpublished observations.

8. Appleman, J. R., and Lienhard, G. E. (1989) *Biochemistry 28*, 8221−7.
9. Lieb, W. R., and Stein, W. D. (1974) *Biochim. Biophys. Acta 373*, 178−196.
10. Hankin, B. L., Lieb, W. R., and Stein, W. D. (1972) *Biochim. Biophys. Acta 288*, 114−126.
11. Baker, G. F., and Widdas, W. F. (1973) *J. Physiol. (London) 231*, 143−165.
12. Baker, G. F., and Naftalin, R. J. (1979) *Biochim. Biophys. Acta 550*, 474−484.
13. Carruthers, A., and Melchior, D. L. (1983) *Biochim. Biophys. Acta 728*, 254−266.
14. Cloherty, E. K., Heard, K. S., and Carruthers, A. (1996) *Biochemistry 35*, 10411−10421.
15. Widdas, W. F. (1980) *Curr. Top. Membr. Transp. 14*, 165−223.
16. Naftalin, R. J., and Holman, G. D. (1977) in *Membrane transport in red cells* (Ellory, J. C., and Lew, V. L., Eds.) pp 257−300, Academic Press, New York.
17. Helgerson, A. L., and Carruthers, A. (1987) *J. Biol. Chem. 262*, 5464−5475.
18. Sultzman, L. A., and Carruthers, A. (1999) *Biochemistry 38*, 6640−6650.
19. Hebert, D. N., and Carruthers, A. (1992) *J. Biol. Chem. 267*, 23829−38.
20. Carruthers, A., and Helgerson, A. L. (1991) *Biochemistry 30*, 3907−15.
21. Hebert, D. N., and Carruthers, A. (1991) *Biochemistry 30*, 4654−4658.
22. Jung, C. Y., Hsu, T. L., Hah, J. S., Cha, C., and Haas, M. N. (1980) *J. Biol. Chem. 255*, 361−4.
23. Sogin, D. C., and Hinkle, P. C. (1978) *J. Supramol. Struct. 8*, 447−453.
24. Lundahl, P., Mascher, E., Andersson, L., Englund, A. K., Greijer, E., Kameyama, K., and Takagi, T. (1991) *Biochim. Biophys. Acta 1067*, 177−86.
25. Casey, J. R., and Reithmeier, R. A. (1993) *Biochemistry 32*, 1172−9.
26. Wellner, M., Monden, I., and Keller, K. (1995) *FEBS Lett. 370*, 19−22.
27. Baker, G. F., and Widdas, W. F. (1988) *J. Physiol. (London) 395*, 57−76.
28. Naftalin, R. J., Smith, P. M., and Roselaar, S. E. (1985) *Biochim. Biophys. Acta 820*, 235−249.
29. Naftalin, R. J., and Rist, R. J. (1991) *Biochim. Biophys. Acta 1064*, 37−48.
30. Jung, C. Y., Carlson, L. M., and Whaley, D. A. (1971) *Biochim. Biophys. Acta 241*, 613−627.
31. Taverna, R. D., and Langdon, R. G. (1973) *Biochim. Biophys. Acta 298*, 422−428.
32. Carruthers, A. (1986) *J. Biol. Chem. 261*, 11028−11037.
33. Hebert, D. N., and Carruthers, A. (1986) *J. Biol. Chem. 261*, 10093−10099.
34. Carruthers, A., and Helgerson, A. L. (1989) *Biochemistry 28*, 8337−8346.
35. Helgerson, A. L., Hebert, D. N., Naderi, S., and Carruthers, A. (1989) *Biochemistry 28*, 6410−6417.
36. Levine, K. B., Cloherty, E. K., Fidyk, N., and Carruthers, A. (1998) *Biochemistry 37*, 12221−12232.
37. Regen, D. M., and Morgan, H. E. (1964) *Biochim. Biophys. Acta 79*, 151−166.
38. Simons, T. J. B. (1983) *J. Physiol. 338*, 477−500.
39. Taylor, L. P., and Holman, G. D. (1981) *Biochim. Biophys. Acta 642*, 325−335.
40. Helgerson, A. L., and Carruthers, A. (1989) *Biochemistry 28*, 4580−4594.
41. Whitesell, R. R., Regen, D. M., Beth, A. H., Pelletier, D. K., and Abumrad, N. A. (1989) *Biochemistry 28*, 5618−5625.
42. Cloherty, E. K., Sultzman, L. A., Zottola, R. J., and Carruthers, A. (1995) *Biochemistry 34*, 15395−15406.
43. Wheeler, T. J., and Hinkle, P. C. (1981) *J. Biol. Chem. 256*, 8907−8914.
44. Heard, K. S., Diguette, M., Heard, A. C., and Carruthers, A. (1998) *Exp. Physiol. 83*, 195−201.
45. Lachaal, M., Berenski, C. J., Kim, J., and Jung, C. Y. (1990) *J. Biol. Chem. 265*, 15449−54.
46. Steck, T. L., and Yu, J. (1973) *J. Supramol. Struct. 1*, 220−232.
47. Weed, R. I., LaCelle, P. L., and Merrill, E. W. (1969) *J. Clin. Invest. 48*, 795−809.
48. Sheetz, M. P., and Singer, S. J. (1977) *J. Cell Biol. 73*, 638−46.
49. Carruthers, A. (1986) *Biochemistry 25*, 3592−3602.
50. Sogin, D. C., and Hinkle, P. C. (1980) *Biochemistry 19*, 5417−5420.
51. Baldwin, S. A., Baldwin, J. M., and Lienhard, G. E. (1982) *Biochemistry 21*, 3836−3842.
52. Rampal, A. L., Jung, E. K., Chin, J. J., Deziel, M. R., Pinkofsky, H. B., and Jung, C. Y. (1986) *Biochim. Biophys. Acta 859*, 135−142.
53. Cloherty, E. K., Diamond, D. L., Heard, K. S., and Carruthers, A. (1996) *Biochemistry 35*, 13231−13239.
54. Diamond, D., and Carruthers, A. (1993) *J. Biol. Chem. 268*, 6437−6444.
55. Simpson, I. A., and Cushman, S. W. (1986) *Annu. Rev. Biochem. 55*, 1059−1089.
56. Laemmli, U. K. (1970) *Nature 227*, 680−685.

BI991931U